Applied Catalysis B: Environmental 210 (2017) 116–120

Contents lists available at ScienceDirect

Applied Catalysis B: Environmental

journal homepage: www.elsevier.com/locate/apcatb

Deactivation mechanism and regeneration of carbon nanocomposite catalyst for acetylene hydrochlorination

Xingyun Li, Pan Li, Xiulian Pan*, Hao Ma, Xinhe Bao

State Key Laboratory of Catalysis, Dalian Institute of Chemical Physics, Chinese Academy of Sciences, Zhongshan Road 457, Dalian 116023, China

ARTICLE INFO

Article history:
Received 31 October 2016
Received in revised form 3 March 2017
Accepted 17 March 2017
Available online 18 March 2017

Keywords:
Acetylene hydrochlorination
Metal free
Carbon catalysis
Carbon deposit
Catalyst regeneration

ABSTRACT

Acetylene hydrochlorination is an important coal-based technology for production of vinyl chloride, the monomer of one of the world mostly used plastics. Despite of the great potentials demonstrated for carbon-based catalysts to replace the toxic mercury chloride, the stability and the deactivation mechanism are rarely discussed, which is essential for real applications. Herein, we present a detailed study on the deactivation mechanism of nitrogen doped carbon based catalyst in acetylene hydrochlorination. The results show that the deactivation was likely caused by the carbon-like deposition over the catalyst, which can be regenerated with high temperature NH_3 treatment.

1. Introduction

Acetylene hydrochlorination is an important coal-based process to produce vinyl chloride, especially for countries rich in coal but deficient in oil resources such as China and India. Vinyl chloride is the monomer of polyvinyl chloride, which is the third mostly used plastics in the world. Mercury chloride ($HgCl_2$) supported on activated carbon (AC) remains the most efficient catalyst up to date. However, $HgCl_2$ is apt to be reduced by acetylene and mercury sublimates under reaction conditions. Furthermore, AC is hard to be shaped and tends to be crushed which accelerates the deactivation of the catalyst. Both the toxicity and limited resources of mercury have prompted wide efforts to explore non-mercury catalysts. For example, a series of metal chlorides, including $PdCl_2$ [1,2], $RuCl_3$ [3,4], K_2PtCl_6 [5], $CuCl_2$-$BiCl_3$ [6] have been investigated as potential mercury-free catalysts. Systematic studies carried out by Hutchings showed that gold chloride may be the best alternative catalyst because of its high activity [7], which is comparable to mercury chloride, although the stability was considered to be an issue. Consequently, intensive efforts have been devoted to improve the stability of gold chloride by adding other metal additives [8–10].

Meanwhile, efforts were made to explore alternative mercury-free catalysts, particularly carbon-based catalysts [11–14]. We reported previously that nitrogen doped carbon can catalyze acetylene hydrochlorination without additional metal catalysts. The acetylene conversion reached 80% and selectivity of vinyl chloride was higher than 98% at 200 °C and space velocity of mixed acetylene and HCl 0.8 ml min^{-1} g^{-1} [11,12]. It was demonstrated that pyrrolic nitrogen bonded with carbon was likely the active site. Despite of the significant progress made in recent years, the stability of carbon-based catalysts is still not satisfactory for real applications, as the activity frequently degraded gradually with time on stream [11–14]. Furthermore, the deactivation mechanism is unclear, and this knowledge is essential for further optimization of catalysts for applications.

It is known that the dopamine molecule can self-polymerize to form polydopamine (PDA) [15], and nitrogen species which are bonded with carbon, form a pyrrolic structure upon polymerization, as shown in Scheme 1 [16]. Therefore, this material may be used as a catalyst for acetylene hydrochlorination [11,12]. More interestingly, PDA can spontaneously adhere strongly onto the surfaces of almost any type of organic or inorganic materials under an alkaline condition. Therefore, we take dopamine as a convenient material for preparation of PDA/SiC nanocomposite by wrapping a layer of PDA material around the SiC substrate. With this, we intend to take advantage of the properties of SiC such as high heat conductivity, good mechanical strength and chemical inertness for applications in hydrochlorination which involves HCl and is strongly exothermal. Thus the deactivation mechanism of carbon-based material is investigated and a possible regeneration method is proposed.

* Corresponding author.
E-mail address: panxl@dicp.ac.cn (X. Pan).

http://dx.doi.org/10.1016/j.apcatb.2017.03.046
0926-3373/

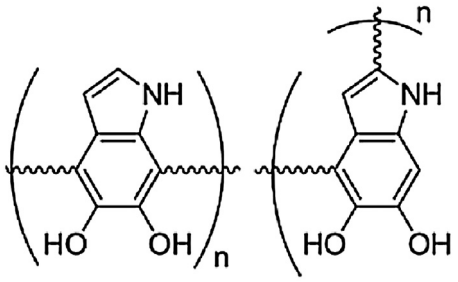

Scheme 1. Possible structure of polymerized dopamine [16].

2. Experimental

2.1. Preparation of PDA

PDA was synthesized following a reported procedure [17]. Typically, 1.5 ml ammonia aqueous solution (30%) was mixed with 50 ml ethanol and 100 ml deionized water. 1.0 g dopamine hydrochloride (Alfa Aesar) was dissolved in 10 ml deionized water and then added to the above solution under stirring. Dopamine was rapidly polymerized, evidenced by the immediate colour change to brown and then to dark black. After further stirring for 30 h to allow complete polymerization, the mixture was filtered and washed with plenty of de-ionized water until the filtrate was neutral. Then PDA was dried in the oven at 60 °C overnight followed by calcination at 600, 800 and 1000 °C in Ar, respectively. The resulting samples were designated as PDA-T, with T representing the calcination temperature.

2.2. Preparation of PDA/SiC

In order to coat the surface of SiC uniformly with PDA, Tris-HCl buffer was used to slow down the polymerization rate to avoid self-polymerization in the bulk forming discrete PDA particles [18]. In brief, 2 g SiC was dispersed in 250 ml Tris-HCl buffer (pH = 8.5) under stirring, and dopamine aqueous solution (4.0 g dopamine hydrochloride dissolved in 100 ml deionized water) was added to the buffer solution, which was stirred for 22 h at room temperature. Then the sample was filtrated and washed repeatedly by water until the filtrate was neutral, and further dried at 110 °C overnight. Following calcination in Ar, the obtained samples were denoted as PDA/SiC-T. Similarly, T represents the calcination temperature (400, 500, 600 and 700 °C, respectively).

2.3. Acetylene hydrochlorination

Acetylene hydrochlorination was carried out in a fixed bed micro-reactor made of quartz. The reaction temperature was set at 200 °C. A mixture of HCl/C_2H_2 with a molar ratio of 1.15 was used as the feeding gas. For the unsupported PDA-derived catalysts, the weight hourly space velocity of the feeding gas was set at 3.1 ml min^{-1} g^{-1}, while for the PDA/SiC derived catalysts, the space velocity was 0.8 ml min^{-1} g^{-1} unless otherwise stated.

2.4. Characterizations

The specific surface areas of the catalysts were measured by nitrogen physisorption at 77 K on a Micromeritics ASAP 2400. The pore size distribution was calculated using a Non-Local Density Functional Theory (NLDFT). The morphology of PDA and PDA/SiC composites was characterized by transition electron microscopy (TEM) on a FEI F30 microscope operated at an acceleration voltage of 200 kV. The surface content of nitrogen species and their structures were analyzed by X-ray photoelectron spectroscopy (XPS) on a VG ESCALAB MK2 spectroscope with Al Kα X-rays as the excitation source at a voltage of 12.5 kV and power of 250 W. Thermogravimetric (TG) analysis was performed on the analyser (Pyris Diamond) in a flowing air at a heating rate of 10 °C/min up to 900 °C.

Table 1
Specific surface area and XPS analysis of the surface composition of PDA-T.

Sample	BET (m^2/g)	N%	O%	Pyrrolic N%[a]
PDA	9.3	7.3	22.3	94.3
PDA-600	204.2	7.3	5.1	59.8
PDA-800	239.5	5.1	5.9	54.1
PDA-1000	98.4	2.3	4.0	7.1

[a] Percentage of pyrrolic N in all N species.

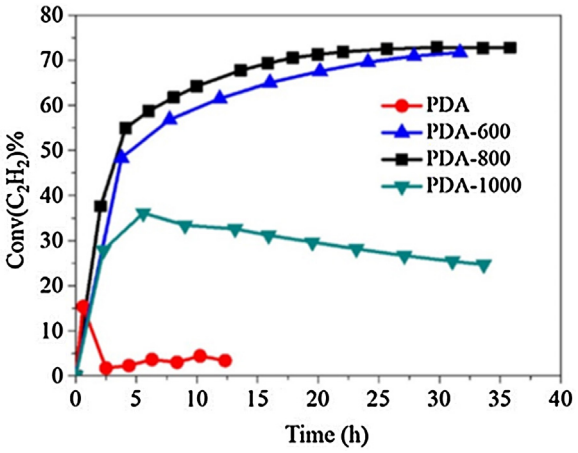

Fig. 1. Catalytic activity of PDA-T in acetylene hydrochlorination. Selectivity to vinyl chloride is above 99% under reaction conditions: 200 °C, HCl/C_2H_2 = 1.15 and space velocity 3.1 ml min^{-1} g^{-1}.

3. Results and discussion

3.1. Properties and catalytic performance of PDA

XPS analysis shows that PDA contains 7.3% nitrogen. As listed in Table 1, 94.3% of these nitrogen species exist as the pyrrolic N structure. However, the activity of PDA is rather low at 200 °C and space velocity of 3.1 ml min^{-1} g^{-1} as shown in Fig. 1. The acetylene conversion is only 15% and it drops rapidly to 3%. This is likely related to the too low surface area of freshly synthesized PDA, which is only 9.3 m^2/g (Table 1). Thus, the active sites may not be efficiently accessible to the reactant molecules although the pyrollic N content is rather high. In addition, PDA contains a high content of oxygen species (about 22.3%) (Table 1), which may also hinder the activation of acetylene, as observed previously [12]. Therefore, we treated PDA at high temperatures in Ar atmosphere. This removes the oxygen containing groups and leads to an increased surface area. For example, the surface area of PDA-600 jumps to 204.2 m^2/g, which is about 22 times that of the original PDA and the oxygen content drops to 5.1%. But this comes at the expense of a reduced amount of the pyrrolic N species (59.8% in PDA-600 vs. 94.3% in PDA) due to the relatively low stability of the pyrrolic N structure [17]. A higher treatment temperature leads to further increased surface area and reduced pyrrolic N content. For example, PDA-800 exhibits an area of 239.5 m^2/g and pyrrolic N content of 54.1%. The oxygen content does not decrease further likely due to the re-adsorption of oxygen-containing groups when the sample is exposed to air before XPS measurement. Consequently, the catalytic activity of PDA-600 and PDA-800 improves significantly with respect to PDA. After reaching a steady state, PDA-600 and PDA-800 exhibit a similar activity, with acetylene conversion rising to about 70% (Fig. 1). However, calcination at 1000 °C is obviously detrimental as acetylene conversion

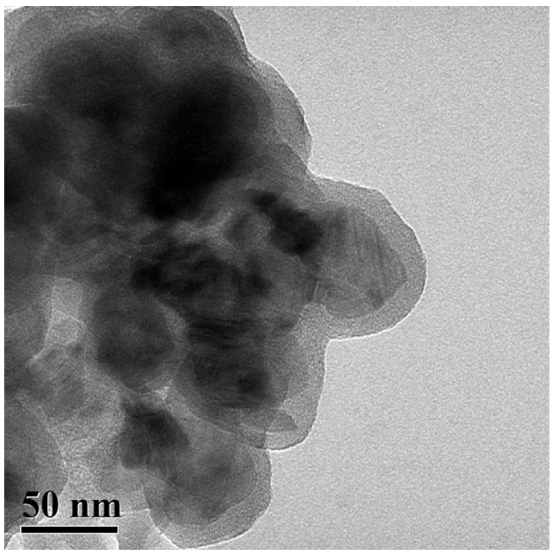

Fig. 2. TEM image of PDA/SiC.

Table 2
Specific surface area and XPS analysis of the surface composition of PDA/SiC-T.

Sample	BET (m^2/g)	N%	O%	Pyrrolic N%[a]
PDA/SiC-400	46.4	6.8	14.2	55.2
PDA/SiC-500	56.4	6.5	9.8	53.7
PDA/SiC-600	60.0	5.0	9.5	53.1
PDA/SiC-700	86.5	4.5	6.9	54.3

[a] Percentage of pyrrolic N in all N species.

drops down to around 30% under the same reaction conditions. This can be attributed to the remarkably reduced surface area (98.4 m^2/g) and also distinctly decreased nitrogen content down to 2.3%. Collapses of the pores upon high-temperature treatment was also frequently reported [19]. The pyrrolic nitrogen structure is also not stable and may undergo decomposition and transformation at 1000 °C [19]. Furthermore, PDA-1000 is much less stable in the reaction than PDA-600 and PDA-800, as the acetylene conversion decreases obviously with time on stream (Fig. 1).

3.2. Property and catalytic performance of PDA/SiC

To study the feasibility of using SiC as a support for nanostructured carbon, PDA is coated on SiC with a shaped morphology. The TEM images in Fig. 2 show that PDA can be uniformly coated on the surface of SiC with a thickness about 11 nm. Table 2 shows that the calcination temperature has a similar effect on the surface area on PDA/SiC-T and oxygen content. The specific surface area increases from 46.4 m^2/g for PDA/SiC-400 to 86.5 m^2/g for PDA/SiC-700 and at the same time the oxygen content lowers to 6.9% for PDA/SiC-700, which is about half that of PDA/SiC-400. Such structure and composition changes have a great influence on the activity.

As shown in Fig. 3, PDA/SiC-400 gives an acetylene conversion of 46% under reaction conditions of 200 °C and 0.8 ml min^{-1} g^{-1}. The acetylene conversion increases stepwise with the treatment temperature up to 600 °C. For example, the conversion reaches 77% over PDA/SiC-600. However, further increasing temperature does not influence the activity anymore, as the catalyst PDA/SiC-700 exhibits a similar activity as PDA/SiC-600. Since the SiC substrate is inert, we also calculate the conversion rate of acetylene based on the weight loading of PDA. This value reaches 0.083 $g_{C2H2}/h/g_{PDA}$ over PDA/SiC-700 (PDA weight loading 22%), whereas it is 0.066 $g_{C2H2}/h/g_{PDA}$ over the unsupported PDA-600 and PDA-800 catalyst. It shows that the use of SiC support even has a benefit of enhancing the activity of PDA.

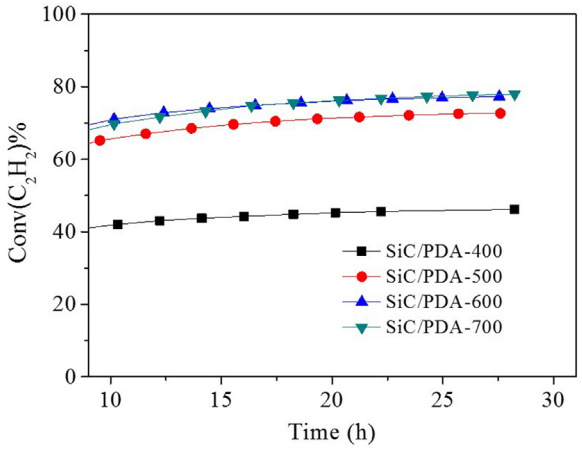

Fig. 3. Catalytic activity of PDA/SiC-T in acetylene hydrochlorination. Selectivity to vinyl chloride is above 99% over studied catalysts. Reaction conditions: 200 °C, HCl/C_2H_2 = 1.15 and space velocity of 0.8 ml min^{-1} g^{-1}.

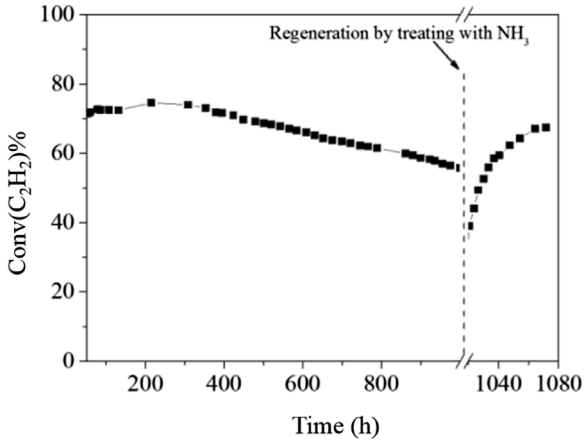

Fig. 4. Stability test of PDA/SiC-700 for a 1000 h and its catalytic activity upon regeneration by high temperature NH_3-treatment. Reaction conditions: 200 °C and space velocity 0.8 ml g^{-1} min^{-1}.

3.3. Deactivation and regeneration of PDA/SiC

We took PDA/SiC-700 as an example to evaluate its long term stability. As shown in Fig. 4, no obvious deactivation is observed during the initial 350 h. However, the conversion of acetylene declines slowly with time on stream after that. After 1000 h, it decreases by 13% with respect to the initial activity. The deactivation of the catalysts is usually caused by the reduction of active sites, either because of leaching, sintering, or transformed structures due to instability, or being poisoned/covered [17]. For the carbon-based catalyst in this study, we do not observe transformation or loss of pyrrolic-structure N species at a relatively low reaction temperature of 200 °C (Table 3). However, active sites might be partially covered during this exothermal reaction because both acetylene and vinyl chloride may oligomerize. For example, acetylene is often used as the precursor for carbon deposition in CVD processes [20–23]. To confirm this, we first carried out TG analysis of the fresh (PDA/SiC-700) and post-reaction catalysts (PDA/SiC-700-p). As shown in Fig. 5, the weight loss increases by about 7% for PDA/SiC-700-p compared with the fresh catalyst, implying the presence of a deposit, which can be removed by air. BET analysis of the post-reaction catalyst (Table 3) shows that both the spe-

Table 3
BET surface area and pore structures of PDA/SiC-700 catalysts.

Sample	BET (m^2/g)	Average pore size[c] (nm)	Pore volume (cc/g)	N%[d]	Cl% [d]
PDA/SiC-700	86.5	6.4	0.25	4.5	0.3
PDA/SiC-700-p[a]	62.2	5.0	0.19	4.3	0.6
PDA/SiC-700-r[b]	84.8	6.3	0.22	4.2	0.3

[a] PDA/SiC-700-p stands for the catalyst after 1000 h stability test.
[b] PDA/SiC-700-r for the one regenerated in NH_3 at 700 °C.
[c] Mean pore size calculated by NL-DFT method.
[d] Estimated from XPS analysis.

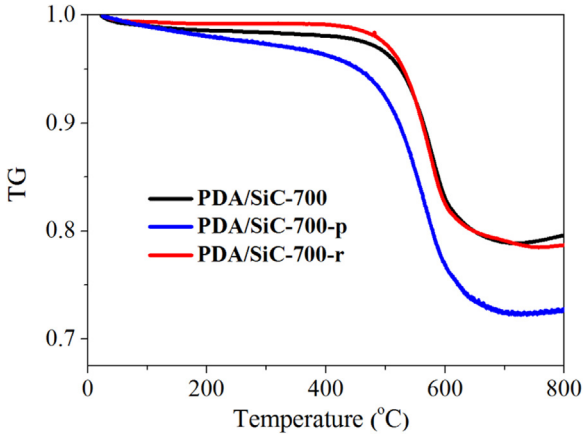

Fig. 5. TG profiles for the fresh, post-reaction and regenerated catalysts of PDA/SiC-700.

cific surface area and pore volume decrease. It indicates that some pores are blocked and/or some surface is covered. XPS shows that the surface concentration of Cl also increases after reaction, which can be attributed to the adsorbed vinyl chloride monomer (VCM) or oligomerized vinyl chloride. Since both acetylene and vinyl chloride may oligomerize, the carbon-like deposit may derive from acetylene and/or vinyl chloride and/or their oligomers under reaction conditions. This will hinder the access of reactants to the active sites, leading to a lowered activity. While it is necessary to further explore catalysts with a higher activity and durability, it is also desirable to develop an effective method to regenerate the catalyst.

The challenge to regenerate carbon-based catalysts lies in effective removal of the surface carbon deposition without damaging its intrinsic carbon network particularly the active sites within the network. Although oxidation in O_2, CO_2 or by reduction in H_2 at high temperatures is a commonly employed method to remove the deposited carbon from the surface of metal or metal oxide catalysts [24–28], it is not applicable for carbon-based catalysts. Our trials show that reduction in hydrogen is also rather difficult to control. Although the carbon deposit can be removed from the catalyst after H_2 treatment at 700 °C, the doped nitrogen species may be also lost partly from the framework of carbon. As a result, the activity of PDA/SiC-700 is not recovered. Therefore, we turned to NH_3 since NH_3 decomposes at high temperatures and can provide hydrogen and nitrogen species at the same time [29,30], which may prevent leaching of nitrogen species in the carbon materials. The TG results in Fig. 5 show that upon regeneration in NH_3 for 1 h at 700 °C, the weight loss drops to the initial level as the fresh catalyst, indicating that the carbon-like deposition can be successfully removed by ammonia. Furthermore, the specific surface area is also restored, as well as the average pore size and the pore volume, as shown in Table 3. XPS demonstrates that the regenerated catalyst contains a similar nitrogen content, suggesting that NH_3 atmosphere does avoid nitrogen leaching during high temperature treatment. After regeneration the conversion of acetylene reaches 72%, similar to the fresh catalyst (Fig. 4). This demonstrates that high temperature NH_3 treatment is an effective way to regenerate the catalyst.

In order to gain deeper insights into the regeneration mechanism, the effluent during the regeneration process in NH_3 was monitored and analyzed by an online mass spectrometer (MS). As shown in Fig. 6, species corresponding to m/e = 27 start to desorb at 150 °C with two maxima at 200 and 300 °C. These species may be attributed to HCN or the fragments of C_2H_3Cl. Since these peaks are also observed in Ar, in which HCN species are not likely to be produced, these low temperature peaks are most likely the dechlorinated fragments of C_2H_3Cl desorbing from the catalyst upon heating. However, these species are not the only reason for the deactivation since just heat-treatment in Ar cannot recover the activity. Fig. 6a shows that the signal corresponding to HCN begins to pick up above 500 °C, and at the same time the NH_3 signal decays above 650 °C. This is likely the result of reaction between the carbon-like deposit with NH_3. In this way, the carbon-like deposit is removed and the activity is restored. However, care has to be taken to remove toxic HCN thoroughly, e.g. by passing the exhaustion through aqueous KOH, and to avoid formation of crystalized

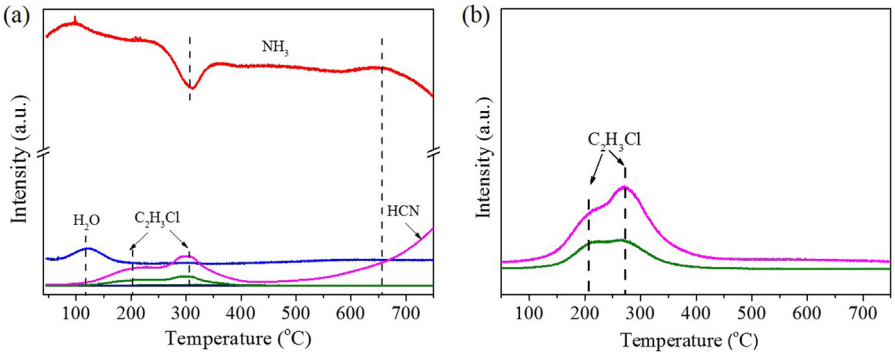

Fig. 6. Effluents during regeneration of PDA/SiC-700-p monitored by an online MS (a) in 6% NH_3 (He balanced); (b) in Ar atmosphere, with m/e = 27 (pink curve) corresponding to HCN and C2H3Cl; with m/e = 62 (green curve) corresponding to C_2H_3Cl; m/e = 18 (blue curve) corresponding to H_2O; and m/e = 17 (red curve) corresponding to NH_3. (For interpretation of the references to colour in this figure legend, the reader is referred to the web version of this article.)

NH_4Cl (reaction of NH_3 with residual HCl in the catalyst) which may block the reactor.

4. Conclusion

This paper demonstrates again that nitrogen-doped carbon can catalyze directly acetylene hydrochlorination to produce vinyl chloride. The results show that it is critical to expose more active sites and to reduce the oxygen content, so as to improve the activity. By coating a layer of PDA around the surface of SiC, we obtain conveniently a composite PDA/SiC, which exhibits a high activity and stability in acetylene hydrochlorination. For example, PDA/SiC-700 gives a conversion of acetylene of 78% at reaction conditions of 200 °C and space velocity 0.8 ml g^{-1} min^{-1}. No obvious deactivation is observed during the initial 350 h time on stream. However, the activity slowly decays and the conversion decreases to 65% after 1000 h. Detailed analysis indicates that carbon-like deposit is likely the reason of deactivation, which blocks the pores and covers the active sites. Regeneration by treatment in NH_3 at 700 °C appears to be an effective approach to recover the activity although further work is still needed to optimize the regeneration process.

Acknowledgement

We acknowledge the financial support of the National Natural Science Foundation of China (grant nos. 21425312, 21321002 and 21373207).

References

[1] Q.L. Song, S.J. Wang, B.X. Shen, J.G. Zhao, Petrol Sci. Technol. 28 (2010) 1825–1833.
[2] J.Y. Hu, Q.W. Yang, L.F. Yang, Z.G. Zhang, B.G. Su, Z.B. Bao, Q.L. Ren, H.B. Xing, S. Dai, ACS Catal. 5 (2015) 6724–6731.
[3] J.L. Zhang, W. Sheng, C.L. Guo, W. Li, RSC Adv. 3 (2013) 21062–21068.
[4] H.Y. Zhang, W. Li, Y.H. Jin, W. Sheng, M.C. Hui, X.Q. Wang, J.L. Zhang, Appl. Catal. B-Environ. 189 (2016) 56–64.
[5] S.A. Mitchenko, E.V. Khomutov, A.A. Shubin, Y.M. Shul'ga, J. Mol. Catal. A-Chem. 212 (2004) 345–352.
[6] K. Zhou, J.C. Jia, X.G. Li, X.D. Pang, C.H. Li, J. Zhou, G.H. Luo, F. Wei, Fuel Process. Technol. 108 (2013) 12–18.
[7] X. Liu, M. Conte, D. Elias, L. Lu, D.J. Morgan, S.J. Freakley, P. Johnston, C.J. Kiely, G.J. Hutchings, Catal. Sci. Technol. 6 (2016) 5144–5153.
[8] H.Y. Zhang, B. Dai, X.G. Wang, W. Li, Y. Han, J.J. Gu, J.L. Zhang, Green Chem. 15 (2013) 829–836.
[9] S.J. Wang, B.X. Shen, Q.L. Song, Catal. Lett. 134 (2010) 102–109.
[10] H.Y. Zhang, B. Dai, X.G. Wang, L.L. Xu, M.Y. Zhu, J. Ind. Eng. Chem. 18 (2012) 49–54.
[11] X.Y. Li, X.L. Pan, X.H. Bao, J. Energy Chem. 23 (2014) 131–135.
[12] X.Y. Li, X.L. Pan, L. Yu, P.J. Ren, X. Wu, L.T. Sun, F. Jiao, X.H. Bao, Nat. Commun. 5 (2014).
[13] K. Zhou, B. Li, Q. Zhang, J.Q. Huang, G.L. Tian, J.C. Jia, M.Q. Zhao, G.H. Luo, D.S. Su, F. Wei, Chemsuschem 7 (2014) 723–728.
[14] M.Y. Zhu, Q.Q. Wang, K. Chen, Y. Wang, C.F. Huang, H. Dai, F. Yu, L.H. Kang, B. Dai, ACS Catal. 5 (2015) 5306–5316.
[15] H. Lee, B.P. Lee, P.B. Messersmith, Nature 448 (2007) U334–U338.
[16] H. Lee, S.M. Dellatore, W.M. Miller, P.B. Messersmith, Science 318 (2007) 426–430.
[17] K.L. Ai, Y.L. Liu, C.P. Ruan, L.H. Lu, G.Q. Lu, Adv. Mater. 25 (2013) 998–1003.
[18] C. Lei, F. Han, D. Li, W.C. Li, Q. Sun, X.Q. Zhang, A.H. Lu, Nanoscale 5 (2013) 1168–1175.
[19] D.H. Deng, X.L. Pan, L.A. Yu, Y. Cui, Y.P. Jiang, J. Qi, W.X. Li, Q.A. Fu, X.C. Ma, Q.K. Xue, G.Q. Sun, X.H. Bao, Chem. Mater. 23 (2011) 1188–1193.
[20] D.L. Plata, E.R. Meshot, C.M. Reddy, A.J. Hart, P.M. Gschwend, Acs Nano 4 (2010) 7185–7192.
[21] D.W. Li, L.J. Pan, Y.K. Wu, W. Peng, Carbon 50 (2012) 2571–2580.
[22] G. Zhong, S. Hofmann, F. Yan, H. Telg, J.H. Warner, D. Eder, C. Thomsen, W.I. Milne, J. Robertson, J. Phys. Chem. C 113 (2009) 17321–17325.
[23] Z.Y. Zeng, J.H. Lin, RSC Adv. 4 (2014) 40251–40258.
[24] Y.M. Zhang, M.Q. Yao, G.G. Sun, S.Q. Gao, G.W. Xu, Ind. Eng. Chem. Res. 53 (2014) 6316–6324.
[25] L.T. dos Santos, F.M. Santos, R.S. Silva, T.S. Gomes, P.M. Esteves, R.D.M. Pimenta, S.M.C. Menezes, O.R. Chamberlain, Y.L. Lam, M.M. Pereira, Appl. Catal. A-Gen. 336 (2008) 40–47.
[26] C. Li, T.C. Brown, Energ. Fuel 13 (1999) 888–894.
[27] C.A. Querini, S.C. Fung, Appl. Catal. A-Gen. 117 (1994) 53–74.
[28] D. Duprez, K. Fadili, J. Barbier, Ind. Eng. Chem. Res. 36 (1997) 3180–3187.
[29] R.P. Lindstedt, F.C. Lockwood, M.A. Selim, Combust. Sci. Technol. 108 (1995) 231–254.
[30] M. Mrowetz, W. Balcerski, A.J. Colussi, M.R. Hoffmann, J. Phys. Chem. B 108 (2004) 17269–17273.